J|A|C|S ARTICLES

Published on Web 05/21/2009

Diffusion-Ordered NMR Spectroscopy in the Structural Characterization of Functionalized Carbon Nanotubes

Riccardo Marega,[†,‡] Vincent Aroulmoji,[‡,¶] Francesca Dinon,[‡] Lisa Vaccari,[§] Silvia Giordani,[||] Alberto Bianco,[⊥] Erminio Murano,[‡,*] and Maurizio Prato[†,*]

Center of Excellence for Nanostructured Materials (CENMAT), Dipartimento di Scienze Farmaceutiche and INSTM UdR Trieste, Università degli Studi di Trieste, Piazzale Europa 1, 34127 Trieste, Italy, Protos Research Institute, Via Flavia 23/1, c/o Sviluppo Italia, 34148, Trieste, Italy, Polymer Conjugation Department, EURAND S.p.A, Area Science Park, Padriciano 99, 34127 Trieste, Italy, Synchrotron ELETTRA Trieste, SISSI beamline, Area Science Park, Basovizza, 34127 Trieste, Italy, School of Chemistry, Center for Research on Adaptive Nanostructures and Nanodevices (CRANN), Trinity College, Dublin, Dublin 2, Ireland, and CNRS, Institut de Biologie Moléculaire et Cellulaire, Laboratoire d'Immunologie et Chimie Thérapeutiques, 67000 Strasbourg, France

Received April 8, 2009; E-mail: prato@units.it; Erminio.Murano@eurand.com

Abstract: The emerging applications of functionalized carbon nanotubes (CNTs) in various research domains necessitate the use of many different analytical techniques to confirm their structural modifications in a fast and reliable manner. Thus far, NMR spectroscopy has not been among the main tools for characterization of organically modified carbon nanostructures. ^{1}H analysis is limited because the signals in these derivatives are typically weak and broad, resulting in uncertainties of a few parts per million, and because of the strong interference of residual solvent signals. To overcome these limitations, we investigated the applicability of proton NMR spectroscopy based on gradient-edited diffusion pulse sequences (1D diffusion-ordered spectroscopy, DOSY) in the characterization of CNT derivatives. In general, diffusion NMR experiments allow the separation of NMR signals of different species present in a mixture, according to their own diffusion coefficients, merging spectroscopy information with size analysis. In the present study, a selected set of CNT derivatives was synthesized and analyzed using 1D DOSY experiments by applying strong magnetic field gradients (up to 42.6 G cm^{-1}). Colorimetric tests (i.e., Kaiser test) and TGA analysis support the NMR findings, which are related to isolated and/or bundled short SWNTs, on the basis of TEM and AFM characterization. The overall results show that the diffusion-based NMR spectroscopy is a fast and promising approach for the characterization of covalently modified CNT derivatives.

Introduction

Carbon nanotubes (CNTs)[1−4] possess extraordinary mechanical, electrical, and optical properties,[5−7] showing great promise[8] in research areas such as high-strength composites,[9] nanosized electronic components,[10,11] and biomedical devices.[12−17] Some of these applications require the solubilization of the pristine CNTs,[18−27] and therefore many covalent and noncovalent

[†] Università degli Studi di Trieste.
[¶] Protos Research Institute.
[‡] EURAND S.p.A.
[§] Synchrotron ELETTRA Trieste.
[||] Trinity College.
[⊥] CNRS.

(1) Iijima, S. *Nature* **1991**, *354*, 56.
(2) Iijima, S.; Ichihashi, T. *Nature* **1993**, *363*, 603.
(3) Subramoney, S.; Ruoff, R. S.; Lorents, D. C.; Malhotra, R. *Nature* **1993**, *366*, 637.
(4) Monthioux, M.; Kutneszov, V. L. *Carbon* **2006**, *44*, 3183.
(5) Saito, R.; Dresselhaus, G.; Dresselhaus, M. S. *Physical Properties of Carbon Nanotubes*; Imperial College Press: London, 1998.
(6) Chen, J.; Hamon, M. A.; Hu, H.; Chen, Y. S.; Rao, A. M.; Eklund, P. C.; Haddon, R. C. *Science* **1998**, *282*, 95.
(7) O'Connell, M. J.; Bachilo, S. M.; Huffman, C. B.; Moore, V. C.; Strano, M. S.; Haroz, E. H.; Rialon, K. L.; Boul, P. J.; Noon, W. H.; Kittrell, C.; Ma, J.; Hauge, R. H.; Weisman, R. B.; Smalley, R. E. *Science* **2002**, *297*, 593.
(8) Baughman, R. H.; Zakhidov, A. A.; De Heer, W. A. *Science* **2002**, *297*, 787.
(9) Lahr, B.; Sandler, J. *Kunstst. Plast. Eur.* **2000**, *90*, 94.
(10) Colbert, D. T.; Smalley, R. E. *Trends Biotechnol.* **1999**, *17*, 46.
(11) White, C. T.; Todorov, T. N. *Nature* **2001**, *411*, 649.
(12) Azamian, B. R.; Davis, J. J.; Coleman, K. S.; Bagshaw, C. B.; Green, M. L. H. *J. Am. Chem. Soc.* **2002**, *124*, 12664.
(13) Lin, Y.; Taylor, S.; Li, H. P.; Fernando, K. A. S.; Qu, L. W.; Wang, W.; Gu, L. R.; Zhou, B.; Sun, Y. P. *J. Mater. Chem.* **2004**, *14*, 527.
(14) Bekyarova, E.; Ni, Y.; Malarkey, E. B.; Montana, V.; McWilliams, J. L.; Haddon, R. C.; Parpura, V. *J. Biomed. Nanotechnol.* **2005**, *1*, 3.
(15) Bianco, A.; Kostarelos, K.; Partidos, C. D.; Prato, M. *Chem. Commun.* **2005**, 571.
(16) Bianco, A.; Hoebeke, J.; Partidos, C. D.; Kostarelos, K.; Prato, M. *Curr. Drug Delivery* **2005**, *2*, 253.
(17) Bianco, A.; Kostarelos, K.; Prato, M. *Expt. Opin. Drug Deliv.* **2008**, *5*, 331.
(18) Bahr, L. J.; Mickelson, E. T.; Bronikowski, M. J.; Smalley, R. E.; Tour, J. M. *Chem. Commun.* **2001**, 193.
(19) Chen, J.; Rao, A. M.; Lyuksyutov, S.; Itkis, M. E.; Hamon, M. A.; Hu, H.; Cohn, R. W.; Eklund, P. C.; Colbert, D. T.; Smalley, R. E.; Haddon, R. C. *J. Phys. Chem. B* **2001**, *105*, 2525.
(20) Niyogi, S.; Hu, H.; Hamon, M. A.; Bhowmik, P.; Zhao, B.; Rozenzhak, S. M.; Chen, J.; Itkis, M. E.; Meier, M. S.; Haddon, R. C. *J. Am. Chem. Soc.* **2001**, *123*, 733.
(21) Sun, Y. P.; Huang, W.; Lin, Y.; Fu, K.; Kitaygorodskiy, A.; Riddle, L. A.; Yu, Y. J.; Carroll, D. L. *Chem. Mater.* **2001**, *13*, 2864.

 10.1021/ja902728w CCC: $40.75

strategies have been developed to this aim.[28,29] The analytical techniques commonly employed to investigate CNTs and CNT derivatives are infrared spectroscopy,[6] Raman spectroscopy,[5,30,31] thermogravimetric analysis (TGA),[32] transmission electron microscopy (TEM), and scanning probe microscopy techniques including atomic force microscopy (AFM) and scanning tunneling microscopy (STM).[33] Since nonfunctionalized CNTs are insoluble in most organic solvents,[18,19] the majority of NMR studies has been performed using ^{13}C-enriched samples by ^{13}C-solid-state analysis.[34−36] This technique was used to understand the mechanism of synthesis and growth of single-walled carbon nanotubes (SWNTs),[34−36] to study gas adsorption mechanisms for energy storage applications,[37−40] to elucidate SWNT dynamics in ropes,[41] and to determine the difference between metallic versus semiconducting SWNTs.[42,43]

^1H NMR analysis of CNTs covalently modified with small organic molecules is limited by the low number of organic functionalities introduced, which improves only slightly the solubility of the derivatives in both organic solvents and aqueous solutions.[29] The addition of carbon radicals to SWNTs[44] and the 1,3-dipolar cycloaddition-mediated attachment of nitrile imines[45] or nitrile oxides[46] or of nitrenes[47] and carbenes[48] to SWNTs sidewalls are some examples of SWNT modification that were investigated by solution ^1H NMR. Some time ago, we characterized the conformation of peptides covalently linked to the sidewalls of SWNTs using 2D NMR spectroscopy.[49] However, it was not possible to observe all the signals, especially those spatially close to the tubes. Recently, another example of 2D NMR, used to characterize 4-mercaptophenyl functionalized SWNTs, was reported.[50] In all the cases, the ^1H NMR interpretation was made particularly difficult by the weakness and broadness of the signals of the attached fragments, often below noise levels: the signals of the molecular fragments become negligible compared to the intensity of the solvent signals, and therefore very long experimental times are needed to obtain structural information.[50] Furthermore, the simple detection of the signals of organic functionalities in the ^1H spectra of CNT derivatives is not a firm proof of covalent conjugation, since a physical mixture[26,51] or an incomplete purification of the derivatives can lead, in principle, to similar results. To overcome these limitations, we investigated the applicability of one-dimensional diffusion-ordered spectroscopy NMR (1D DOSY)[52] for fast and reliable detection of covalent modification on SWNT derivatives. This technique allows separation of NMR signals from species of different size (hydrodynamic radius) exploiting the differences in their apparent diffusion coefficients[53] and was initially developed for the analysis and characterization of complex mixtures and aggregates without purification.[54,55] In a typical DOSY experiment, a series of spectra are recorded with incremented pulsed-field gradient amplitudes in a pulsed-field gradient spin−echo or a pulsed field gradient stimulated spin−echo experiment.[54] DOSY is becoming a popular technique for the determination of molecular weight distribution and structural characterization of polymer mixtures or blends,[56] for the identification of low molecular weight process-related impurities formed during polymer synthesis,[57] and for the study of intermolecular interactions.[58,59] In recent years, DOSY analysis has also been employed for the characterization of nanosized materials such as dendrons,[60−62] fullerenes,[63] and nanoparticles,[64−67] with the

(22) Zhao, B.; Hu, H.; Niyogi, S.; Itkis, M. E.; Hamon, M. A.; Bhowmik, P.; Meier, M. S.; Haddon, R. C. *J. Am. Chem. Soc.* **2001**, *123*, 11673.
(23) Chattopadhyay, D.; Lastella, S.; Kim, S.; Papadimitrakopoulos, F. *J. Am. Chem. Soc.* **2002**, *124*, 728.
(24) Wang, S.; Delduco, D. F.; Lustig, S. R.; Wang, H.; Parker, K. N.; Rizzo, N. W.; Subramoney, S.; Jagota, A.; Humphreys, E. S.; Chung, S.-Y.; Chiang, Y.-M. *Nat. Mater.* **2003**, *2*, 196.
(25) Zhang, J.; Lee, J.-K.; Wu, Y.; Murray, R. W. *Nano Lett.* **2003**, *3*, 403.
(26) Nakashima, N.; Tomonari, Y.; Murakami, H. *Chem. Lett.* **2002**, *31*, 638.
(27) Prato, M.; Kostarelos, K.; Bianco, A. *Acc. Chem. Res.* **2008**, *41*, 60.
(28) Niyogi, S.; Hamon, M. A.; Hu, H.; Zhao, B.; Bhowmik, P.; Sen, R.; Itkis, M. E.; Haddon, R. C. *Acc. Chem. Res.* **2002**, *35*, 1105.
(29) Tasis, D.; Tagmatarchis, N.; Bianco, A.; Prato, M. *Chem. Rev.* **2006**, *106*, 1105.
(30) Kukovecz, A.; Kramberger, C.; Georgakilas, V.; Prato, M.; Kuzmany, H. *Eur. Phys. J. B* **2002**, *28*, 223.
(31) Campidelli, S.; Meneghetti, M.; Prato, M. *Small* **2007**, *3*, 1672.
(32) Landi, B. J.; Cress, C. D.; Evans, C. M.; Raffaelle, R. P. *Chem. Mater.* **2005**, *17*, 6819.
(33) Bonifazi, D.; Nacci, C.; Marega, R.; Campidelli, S.; Ceballos, G.; Modesti, S.; Meneghetti, M.; Prato, M. *Nano Lett.* **2006**, *6*, 1408.
(34) Perez-Cabero, M.; Rodriguez-Ramos, I.; Overweg, A. R.; Sobrados, I.; Sanz, J.; Guerrero-Ruiz, A. *Carbon* **2005**, *43*, 2631.
(35) Urban, M.; Konya, Z.; Mehn, D.; Kiricsi, I. R. *J. Mol. Struct.* **2005**, *744*, 93.
(36) Blackburn, J. L.; Yan, Y.; Engtrakul, C.; Parilla, P. A.; Jones, K.; Gennet, T.; Dillon, A. C.; Heben, M. J. *Chem. Mater.* **2006**, *18*, 2558.
(37) Geng, H. Z.; Zhang, X. B.; Mao, S. H.; Kleinhammes, A.; Shimoda, H.; Wu, Y.; Zhou, O. *Chem. Phys. Lett.* **2004**, *399*, 109.
(38) Matsuda, K.; Hibi, T.; Kadowaki, H.; Kataura, H.; Maniwa, Y. *Phys. Rev. B: Condens. Matter* **2006**, 74.
(39) Mao, S. H.; Kleinhammes, A.; Wu, Y. *Chem. Phys. Lett.* **2006**, *421*, 513.
(40) Clewett, C. F. M.; Pietrass, T. *J. Phys. Chem. B* **2005**, *109*, 17907.
(41) Goze Bac, C.; Latil, S.; Vaccarini, L.; Bernier, P.; Gaveau, P.; Tahir, S.; Micholet, V.; Aznar, R.; Rubio, A.; Metenier, K.; Beguin, F. *Phys. Rev. B: Condens. Matter* **2001**, *63*, 100302.
(42) Tang, X. P.; Kleinhammes, A.; Shimoda, H.; Fleming, L.; Bonnoune, K. Y.; Bower, C.; Zhou, O.; Wu, Y. *Science* **2000**, *288*, 492.
(43) Kitaygorodskiy, A.; Wang, W.; Xie, S. Y.; Lin, Y.; Fernando, K. A. S.; Wang, X.; Qu, L. W.; Chen, B.; Sun, Y. P. *J. Am. Chem. Soc.* **2005**, *127*, 7517.
(44) Umek, P.; Seo, J. W.; Hernadi, K.; Mrzel, A.; Pechy, P.; Mihailovic, D. D.; Forro, L. *Chem. Mater.* **2003**, *15*, 4751.
(45) Alvaro, M.; Atienzar, P.; de la Cruz, P.; Delgado, J. L.; Garcia, H.; Langa, F. *J. Phys. Chem. B* **2005**, *108*, 12691.
(46) Alvaro, M.; Atienzar, P.; de la Cruz, P.; Delgado, J. L.; Troiani, V.; Garcia, H.; Langa, F.; Palkar, A.; Echegoyen, L. *J. Am. Chem. Soc.* **2006**, *128*, 6626.
(47) Holzinger, M.; Abraha, J.; Whelan, P.; Graupner, R.; Ley, L.; Hennrich, F.; Kappes, M.; Hirsch, A. *J. Am. Chem. Soc.* **2003**, *125*, 8566.
(48) Yinghuai, Z.; Peng, A. T.; Carpenter, K.; Maguire, J. A.; Hosmane, N. S.; Takagaki, M. *J. Am. Chem. Soc.* **2005**, *127*, 9875.
(49) Pantarotto, D.; Partidos, C. D.; Graff, R.; Hoebeke, J.; Briand, J. P.; Prato, M.; Bianco, A. *J. Am. Chem. Soc.* **2003**, *125*, 6160.
(50) Nelson, D. J.; Rhoads, H.; Brammer, C. *J. Phys. Chem. C* **2007**, *111*, 17872.
(51) Li, H.; Zhou, B.; Lin, Y.; Gu, L.; Wang, W.; Fernando, K. A. S.; Kumar, S.; Allard, L. F.; Sun, Y. P. *J. Am. Chem. Soc.* **2004**, *126*, 1014.
(52) Loening, M. N.; Keeler, J.; Morris, G. A. *J. Magn. Reson.* **2001**, *153*, 103.
(53) Nilsson, M.; Connell, M. A.; Davis, A. L.; Morris, G. A. *Anal. Chem.* **2006**, *78*, 3040.
(54) Morris, K. F.; Johnson, C. S. *J. Am. Chem. Soc.* **1992**, *112*, 3139.
(55) Viel, S.; Capitani, D.; Mannina, L.; Segre, A. *Biomacromolecules* **2003**, *4*, 1843.
(56) Callaghan, P. T.; Pinder, D. N. *Macromolecules* **1988**, *16*, 968.
(57) Kellenbach, E.; Burgering, M.; Kaspersen, F. *Org. Process Res. Dev.* **1999**, *3*, 141.
(58) Kapur, G. S.; Cabrita, E. J.; Berger, S. *Tetrahedron Lett.* **2000**, *41*, 7181.
(59) Viela, S.; Mannina, L.; Segre, A. *Tetrahedron Lett.* **2002**, *43*, 2515.
(60) Gabriel, C. J.; DeMatteo, M. P.; Paul, N. M.; Takaya, T.; Gustafson, T. L.; Hadad, C. M.; Parquette, J. R. *J. Org. Chem.* **2006**, *71*, 9035.
(61) Ornelas, C.; Boisselier, E.; Martinez, V.; Pianet, I.; Ruiz Aranzaes, J.; Astruc, D. *Chem. Commun.* **2007**, 5093.
(62) Rudzevich, Y.; Rudzevich, V.; Moon, C.; Brunklaus, G.; Böhmer, V. *Org. Biomol. Chem.* **2008**, *6*, 2270.
(63) Zhu, Y. Y.; Li, C.; Li, G. Y.; Jiang, X. K.; Li, Z. T. *J. Org. Chem.* **2008**, *73*, 1745.

Scheme 1 [a]

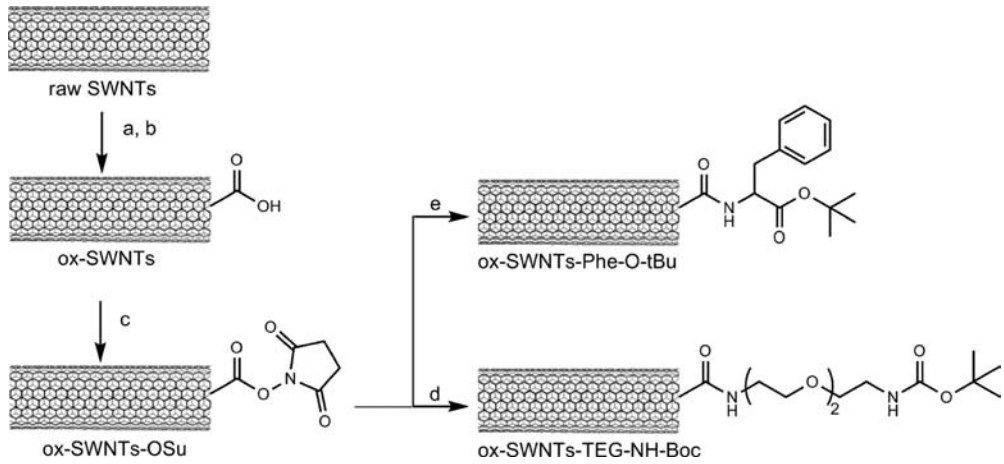

[a] (a) 2.6 M HNO_3 reflux for 48 h, (b) piranha solution (H_2SO_4−30% H_2O_2 4:1), 35 °C, (c) *N*-hydroxysuccinimide (NHS), ethyl-dimethylaminopropyl carbodiimide hydrochloride (EDC·HCl), and 4-dimethylaminopyridine (DMAP) in DMF, (d) Boc-NH-TEG-NH_2, (e) HCl·H-Phe-O-*t*Bu.

aim of understanding size changes and/or intermolecular forces with organic molecules. Here, we propose the use of DOSY as a technique to evaluate the covalent conjugation of small organic fragments to CNTs. When a small organic molecule is covalently linked to a macromolecule, its diffusion coefficient becomes very similar to that of the macromolecular species,[68,69] and therefore, in the spectrum obtained with gradients, the signals of the rapidly diffusing unconjugated molecules are strongly attenuated and become practically negligible. The signal intensity of the more slowly diffusing macromolecular conjugates is also attenuated but the effect is less marked. A small set of CNT derivatives covalently linked via amide bond to organic amines was prepared starting from oxidized SWNTs (ox-SWNTs).[33] These derivatives show moderate dispersability in some organic solvents such as chloroform, dimethylformamide, and dimethyl sulfoxide (DMSO) and were thus suitable for NMR analysis in deuterated solvents. The comparison between ^{1}H and DOSY spectra, along with other indirect evidence (i.e., Kaiser test), allowed us to exclude ionic interactions or physisorption phenomena between ox-SWNTs and amines and to obtain structural information of the functionalized ox-SWNTs. TGA was used to estimate the degree of ox-SWNT functionalization. Finally, TEM and AFM characterization of the solubilized ox-SWNTs derivatives confirmed the presence of bundled and isolated short SWNTs.

Results and Discussion

HiPco SWNTs were oxidized by a two-step procedure previously reported.[33] The carboxylic groups of ox-SWNTs were then activated as *N*-hydroxysuccinimidyl esters (ox-SWNTs-OSu)[29] and subsequently allowed to react in DMF with three organic amines to form amides. The amines used were L-phenylalanine-*tert*-butyl ester (H-Phe-O-*t*Bu) and the Boc-monoprotected derivative of the bis-amino-triethyleneglycol (Boc-NH-CH_2CH_2-$(OCH_2CH_2)_2$-NH_2, **Boc-NH-TEG-NH_2**) to obtain **ox-SWNT-Phe-O-*t*Bu** and **ox-SWNT-TEG-NH-Boc**, respectively (Scheme 1).

The two functionalizing moieties were chosen for conjugation with the **ox-SWNTs** to give derivatives soluble in organic solvents thus suitable for NMR analysis and characterized by a set of signals (*tert*-butyl and phenyl groups) in regions of the spectrum free from solvent interference. In addition, both amino- and carboxy-protecting groups can be easily removed allowing further functionalization. After conjugation, the excess amine was removed by aqueous workup. The purification procedure takes advantage of the different solubility of the amines and the ox-SWNTs conjugates in the same solvent: the ox-SWNT derivatives are insoluble in Et_2O and H_2O and were isolated from DMF dispersion following two subsequent precipitations in Et_2O (first step) and H_2O (second step). Finally, filtration through poly(tetrafluoroethylene) 0.2-μm filters followed by thorough washing yielded the desired products as black powders.

Complete removal of unreacted amines was assessed by ninhydrin assay (qualitative Kaiser test). Using this colorimetric assay, it is possible to quickly detect the presence of primary amines in both solution- and solid-state samples (a blue to blue-violet color is given by α-amino acids and constitutes a positive test); after two purification cycles the assay indicated complete absence of free amino groups. The samples were then subjected to thermogravimetric analysis to quantify the degree of functionalization of the ox-SWNTs derivatives after conjugation. Figure 1 reports the temperature-modulated and the differential thermal plots obtained after a slow temperature scan (temperature increment of 5 °C min^{-1}) of **ox-SWNTs**, HCl·H-Phe-O-*t*Bu, **ox-SWNT-TEG-NH-Boc**, and **ox-SWNT-Phe-O-*t*Bu**, respectively, carried out under nitrogen.

The differential thermal plots allow the determination of the temperature range within which the pyrolysis processes occur. The **ox-SWNTs** differential thermal plot (Figure 1a) shows a main weight loss in the range between 125 and 380 °C due to decarboxylation processes. The associated weight loss (∼15%) indicates an amount of 3.4 μmol mg^{-1} of carboxylic groups for the **ox-SWNTs** samples, corresponding to an average of one carboxylic group every 20 carbon atoms. The **ox-SWNT-Phe-O-*t*Bu** differential thermal plot (Figure 1d) presents two

(64) Durand, J.; Fernández, F.; Barrière, C.; Teuma, E.; Gómez, K.; González, G.; Gómez, M. *Magn. Reson. Chem.* **2008**, *46*, 739.
(65) Evangelisti, C.; Raffa, P.; Balzano, F.; Barretta, G. U.; Vitulli, G.; Salvadori, P. *J. Nanosci. Nanotechnol.* **2008**, *8*, 2096.
(66) Fielden, J.; Long, D. L.; Slawin, A. M. Z.; Kögerler, P.; Cronin, L. *Inorg. Chem.* **2007**, *46*, 9090.
(67) Van Lokeren, L.; Maheut, G.; Ribot, F.; Escax, V.; Verbruggen, I.; Sanchez, C.; Martins, J. C.; Biesemans, M.; Willem, R. *Chem.−Eur. J.* **2007**, *13*, 6957.
(68) Sorbi, C.; Bergamin, M.; Bosi, S.; Dinon, F.; Aroulmoji, V.; Khan, R.; Murano, E.; Norbedo, S. *Carbohydr. Res.* **2009**, *344*, 91.
(69) Norbedo, S.; Dinon, F.; Bergamin, M.; Bosi, S.; Aroulmoji, V.; Khan, R.; Murano, E. *Carbohydr. Res.* **2009**, *344*, 98.

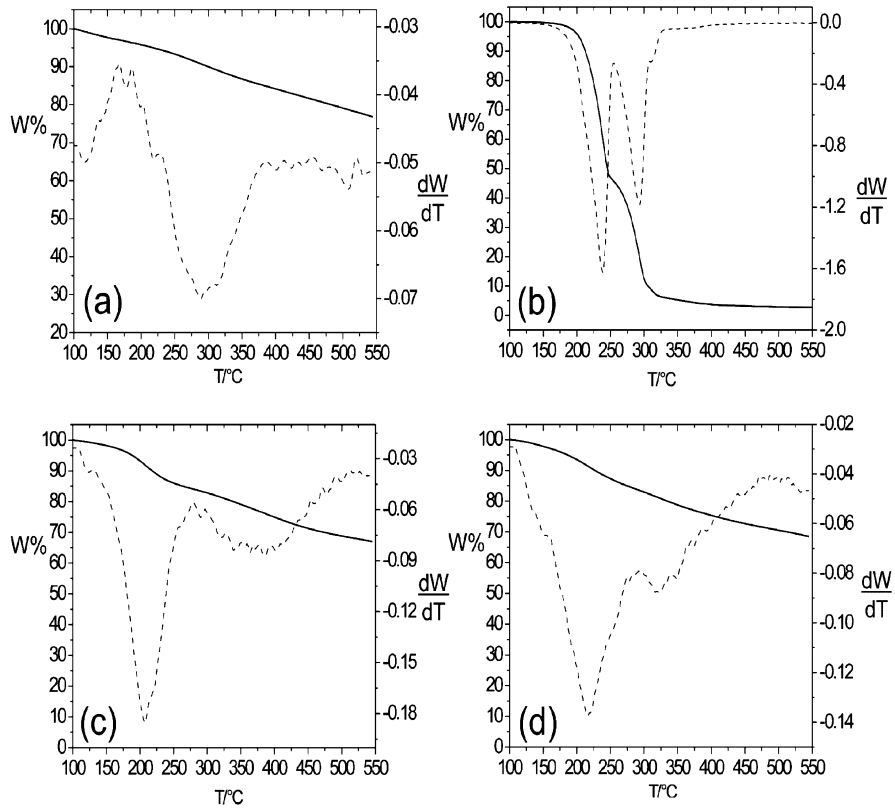

Figure 1. Temperature-modulated plots (—) and differential thermal plots (– – –) of (a) **ox-SWNTs** (1.720 mg), (b) HCl·H-Phe-O-*t*Bu (2.731 mg), (c) **ox-SWNT-TEG-NH-Boc** (2.954 mg), and (d) **ox-SWNT-Phe-O-*t*Bu** (1.732 mg), recorded under N_2 flow (20 mL min^{-1}) with a temperature increase of 5 °C min^{-1}.

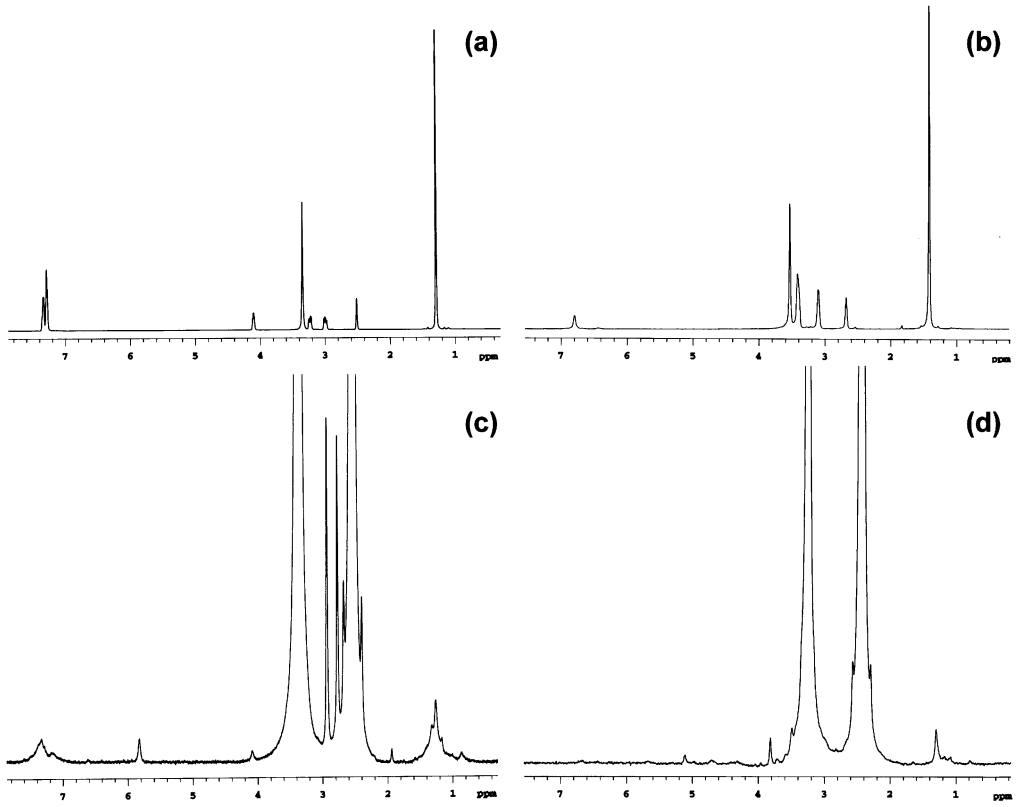

Figure 2. ^{1}H NMR spectra of (a) HCl·H-Phe-O-*t*Bu, (b) Boc-NH-TEG-NH_2, (c) **ox-SWNT-Phe-O-*t*Bu**, and (d) **ox-SWNT-TEG-NH-Boc**.

decomposition events, the first between 120 and 275 °C (around 15% of weight loss) and the second between 280 and 450 °C (overall weight loss = 27.5%). The **ox-SWNT-TEG-NH-Boc** derivative shows the same behavior (Figure 1c), with the first

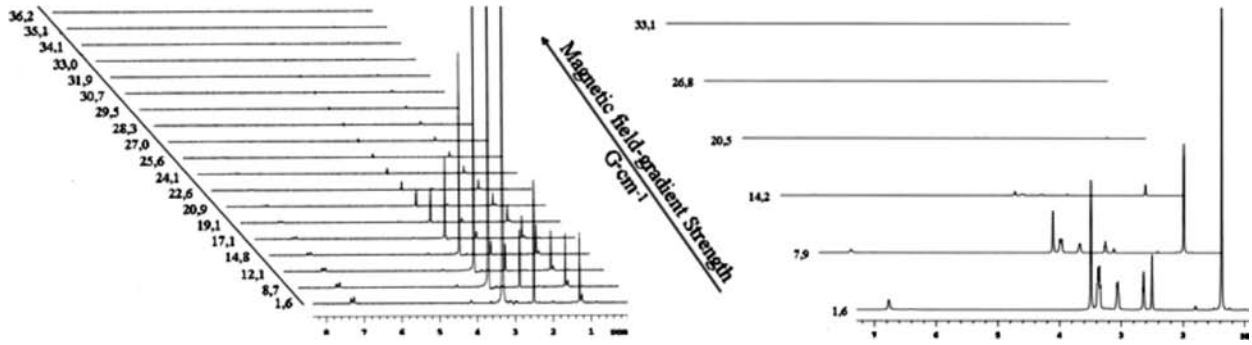

Figure 3. 1D DOSY-arrayed spectra of d_6-DMSO solutions of HCl·H-Phe-O-*t*Bu (with 19 increments of magnetic field gradient from 1.6 to 36.2 G cm^{-1}, left) and Boc-NH-TEG-NH$_2$ (with six increments from 1.6 to 33.1 G cm^{-1}, right).

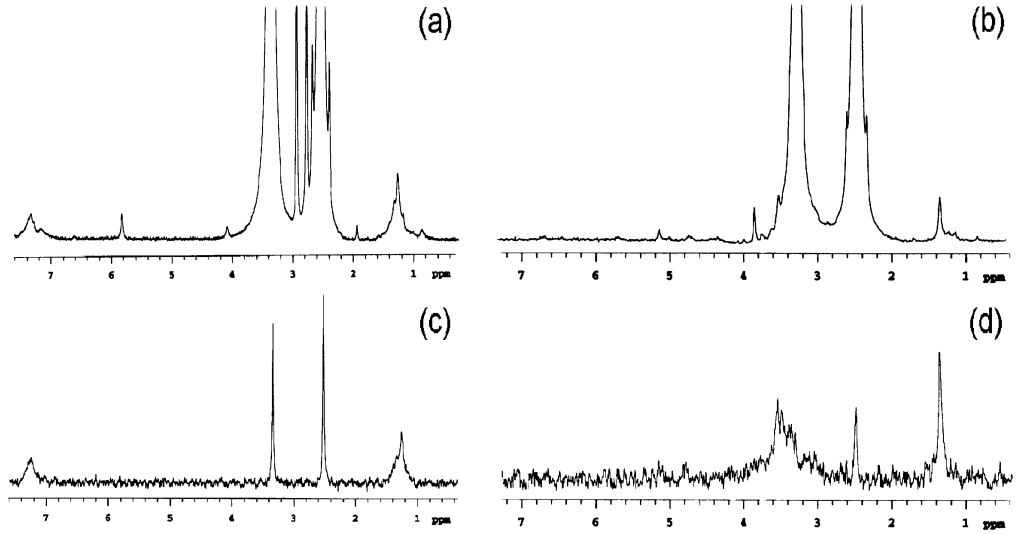

Figure 4. ^{1}H NMR spectra of (a) **ox-SWNT-Phe-O-*t*Bu**, and (b) **ox-SWNT-TEG-NH-Boc**, 1D DOSY spectra of (c) **ox-SWNT-Phe-O-*t*Bu** at 36.5 G cm^{-1}, and (d) **ox-SWNT-TEG-NH-Boc** at 42.6 G cm^{-1}.

pyrolysis occurring between 120 and 275 °C (16% of weight loss) and the second between 276 and 480 °C (overall weight loss = 30%). For both derivatives, it is probable that the first decomposition represents the overlap of ox-SWNT partial decarboxylation and the *tert*-butyl protecting group pyrolysis. It is well-known that the latter functionality can be thermally cleaved from the protected derivatives, especially when the temperature rises above 130 °C.[70] According to this set of data, a functionalization degree of 1.0 and 1.1 μmol mg^{-1} was estimated for **ox-SWNT-Phe-O-*t*Bu** and **ox-SWNT-TEG-NH-Boc**, respectively. In support of this assumption, the starting amine, for example HCl·H-Phe-O-*t*Bu (Figure 1b), shows a two-step weight loss, due to the differential pyrolysis of the *tert*-butyl ester and of the amino acid residue. According to this reasoning, the yield of amide bond formation is about 30% (Figure S1 in the Supporting Information), acceptable for a diimide-mediated coupling on SWNTs.[71]

According to the TGA data, the loading of organic functionalities attached to ox-SWNTs is very low, which requires very sensitive analytical techniques for their structural characterization. Usually microscopy-based techniques with atomic-scale resolution, such as STM,[33] HR-TEM, and Z-STEM,[72] are used to confirm the presence of functionalities along the CNT structure. Nevertheless, the objective of the present study was to establish the covalent derivatization of ox-SWNTs using NMR spectroscopy and then correlate the resulting data with microscopy-based identification of CNTs in the samples. The solubility of **ox-SWNT-Phe-O-*t*Bu** and **ox-SWNT-TEG-NH-Boc** in DMSO, determined by the method described by Holzinger et al.,[47] resulted in 0.88 and 0.83 mg mL^{-1}, respectively. Therefore, all the samples were subjected to ^{1}H NMR analysis in d_6-DMSO. ^{1}H spectra of the CNT conjugates and the corresponding amines are reported in Figure 2.

As expected, the low solubility of the CNT derivatives resulted in spectra characterized by a strong solvent interference (DMSO 2.50 ppm and H_2O 3.30 ppm) whose signals hide some signals of the amine moieties. However, in the **ox-SWNT-Phe-O-*t*Bu** spectrum, the two broad and relatively intense signals of *t*-butyl group at 1.28 ppm and of phenyl ring at 7.23 ppm are clearly visible in the spectrum regions free from interference, with an approximate integration ratio of 9 to 5 (Figure S2 in the Supporting Information). The signal broadening observed is the result of two well-known effects: (i) T_2 relaxation time modification due to the conjugation to a macromolecule,[71] and (ii) the influence of the nonhomogeneous sidewall and tip

(70) Greene, T. W.; Wuts, P. G. M. *Protective Groups in Organic Synthesis*; Wiley & Sons: New York, 1999.
(71) Huang, W.; Fernando, K. A. S.; Allard, L. F.; Sun, Y. P. *Nano Lett.* **2003**, *3*, 565.
(72) Accorsi, G.; Armaroli, N.; Parisini, A.; Meneghetti, M.; Marega, R.; Prato, M.; Bonifazi, D. *Adv. Funct. Mater.* **2007**, *17*, 2975.

structural properties of SWNT on the local magnetic field of the conjugated amines.[47] The **ox-SWNT-TEG-NH-Boc** spectrum shows the *t*-butyl group signal at 1.30 ppm, while the signals of oligoethyleneglycol chain are completely hidden by the peaks of the solvent. The ox-SWNT derivatives were then subjected to DOSY experiments to verify the suitability of the technique for the characterization of CNT conjugates. DOSY is a pulsed-field gradient NMR experiment used to evaluate diffusive behavior of molecules in solution. A typical DOSY experiment consists of a diffusion delay, flanked by two pulse-field gradients. The first gradient labels the position and the order of individual spins of the molecules in the sample. This label is then removed by the second gradient pulse, referred to as the refocusing gradient. If the spins remain stationary during the time between the gradient pulses, as in the case of slowly moving molecules, the intensity and phase of the NMR signal after the refocusing gradient will be independent of the strength and length of the gradient pulses. If the spins move between the phase labeling and the refocusing gradients, as in the case of fast moving molecules, the intensity and/or phase of the signal will be affected. According to theory,[73] the NMR spectrum will show strongly attenuated signals from rapidly diffusing, small molecules, while slowly diffusing, large macromolecules will show less attenuated signals. The ox-SWNTs used in this study have an average length of 180 nm (as determined by STM) and an estimated average diameter larger than 0.9 nm (as determined by Raman spectroscopy and STM),[33] and thus it was expected that the difference of molecular size results in a marked difference in diffusion coefficients between the two interacting species (i.e., amines and CNTs). Field-gradient strength and delay time at which complete attenuation of free amine signals occurs during the DOSY experiment were assessed before the analysis of conjugates. Solutions (~4 mM, 1 mg mL^{-1}) of free amines were subjected to an array of pulsed gradients, as reported in Figure 3. Absolute intensity analysis indicated that, for field gradients higher than 34.1 G cm^{-1} for HCl·H-Phe-O-*t*Bu and 26.8 G cm^{-1} for Boc-NH-TEG-NH_2 free amine signals are completely attenuated and disappear under noise level.

The solubility in d_6-DMSO of **ox-SWNT-Phe-O-*t*Bu** and **ox-SWNT-TEG-NH-Boc** derivatives is less than 0.9 mg mL^{-1}, corresponding to a concentration of approximately 0.9 mM with respect to the attached amines, while the solutions of starting amines used for optimizing the DOSY parameters were 4 mM. This means that the solutions used to assess DOSY parameters contain a higher concentration of amines than those attached to ox-SWNT derivatives employed in the NMR characterization.

Once the DOSY parameters are set, **ox-SWNT-Phe-O-*t*Bu** and **ox-SWNT-TEG-NH-Boc** were analyzed under the same conditions. Figure 4c,d reports their 1D DOSY spectra edited after 512 transients.

In both spectra, the signals of linked amines are present and the solvent signals are attenuated, as compared to the corresponding ^{1}H spectra. In the **ox-SWNT-Phe-O-*t*Bu** spectrum (Figure 5c), signals of αCH and βCH_2 protons of phenylalanine suffer of a poor signal-to-noise ratio due to the low functionalization and solubility of the conjugate, and only the more intense signals of *t*-butyl ester and aromatic ring of phenylalanine are clearly visible. In the **ox-SWNT-TEG-NH-Boc** spectrum, the attenuation of the solvent signals revealed the broad multiplet of triethyleneglycol chain centered at 3.5 ppm (Figure 4d). The characterizations were performed on several batches, affording reproducible results (see also Figure S3 in the Supporting Information). To confirm the covalent attachment of the amines to the nanotubes, we compared the ^{1}H and 1D DOSY spectra of **ox-SWNT-Phe-O-*t*Bu** with those obtained by mixing **oxSWNTs** and HCl·H-Phe-O-*t*Bu, without using coupling reagents, on the basis of the amount of functional groups determined by TGA (Figure 5a,b). Despite the prolonged sonication between **ox-SWNTs** and HCl·H-Phe-O-*t*Bu in d_6-DMSO, it was not possible to achieve the same solubilization of the nanotubes as in the case of the covalent conjugates.

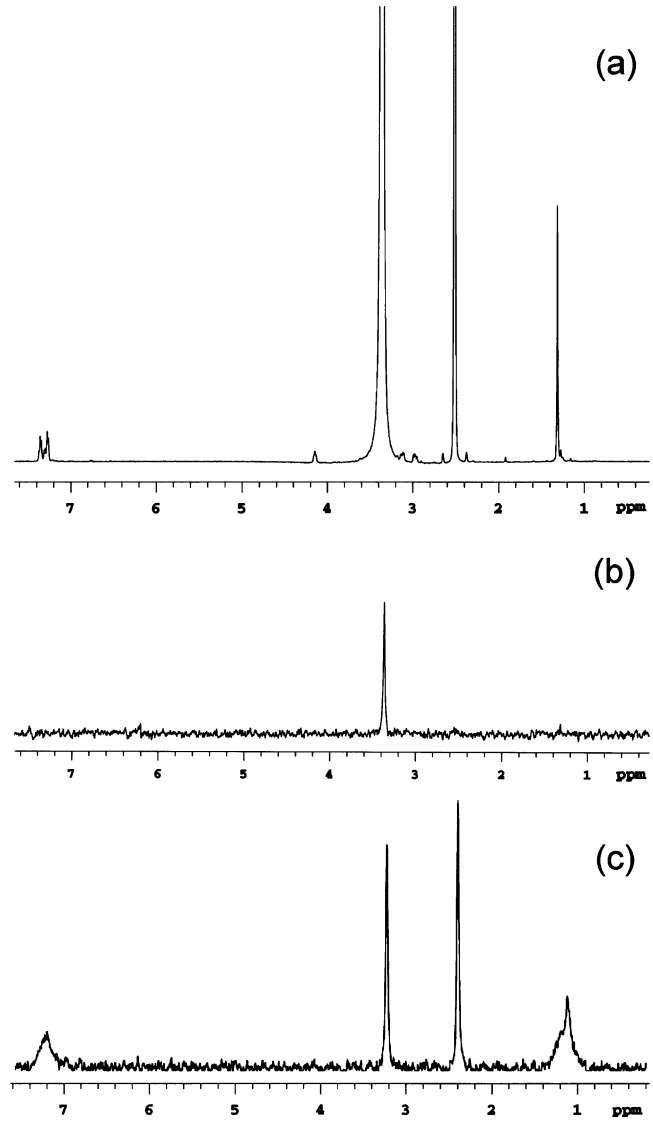

Figure 5. (a) ^{1}H NMR and (b) 1D DOSY spectra of the mixture of **ox-SWNTs** and HCl·H-Phe-O-*t*Bu at 36.5 G cm^{-1}, and (c) 1D DOSY spectra of **ox-SWNTs-Phe-*t*Bu** at 36.5 G cm^{-1}.

The ^{1}H NMR spectra of the mixture show the sharp signals of the HCl·H-Phe-O-*t*Bu, but in the 1D DOSY spectra, recorded under the same conditions employed for **ox-SWNT-Phe-O-*t*Bu**, those signals disappear (Figure 5). Even if HCl·H-Phe-O-*t*Bu were associated to the **ox-SWNTs** in a zwitterionic form, or via hydrogen bond, the weak interactions allow a fast exchange

(73) Stejskal, E. O.; Tanner, J. E. *J. Chem. Phys.* **1965**, *42*, 288.
(74) Kordatos, K.; Da Ros, T.; Bosi, S.; Vazquez, E.; Bergamin, M.; Cusan, C.; Pellarini, F.; Tomberli, V.; Baiti, B.; Pantarotto, D.; Georgakilas, V.; Spalluto, G.; Prato, M. *J. Org. Chem.* **2001**, *66*, 4915.
(75) Horcas, I.; Fernandez, R.; Gomez-Rodriguez, J. M.; Colchero, J.; Gomez-Herrero, J.; Baro, A. M. *Rev. Sci. Instrum.* **2007**, *78*, 013705.

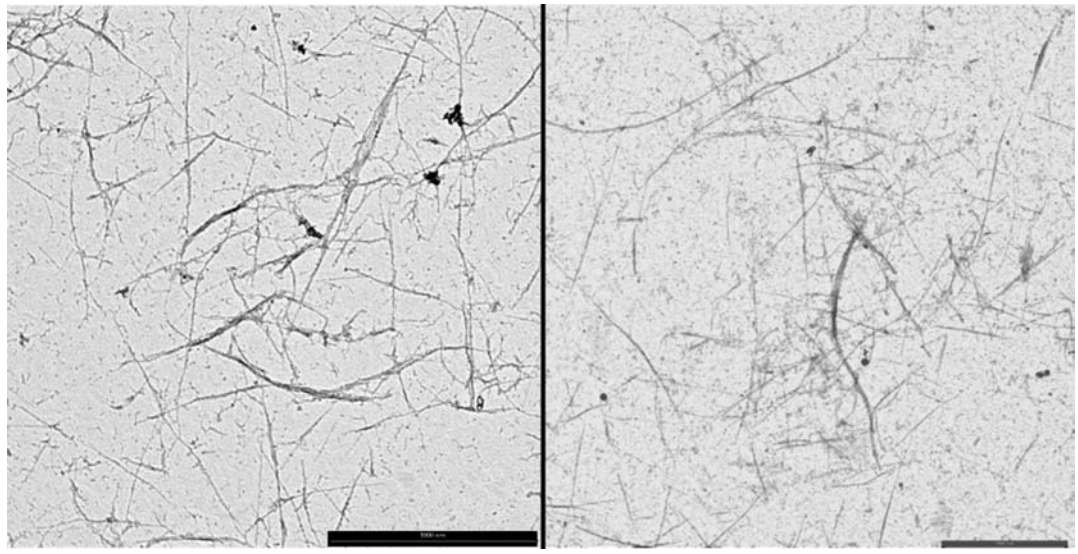

Figure 6. TEM micrographs of **ox-SWNT-Phe-O-*t*Bu** (left) and **ox-SWNT-TEG-NH-Boc** (right) deposited on Cu grids from d_6-DMSO-saturated solutions. Scale bars are 1 μm.

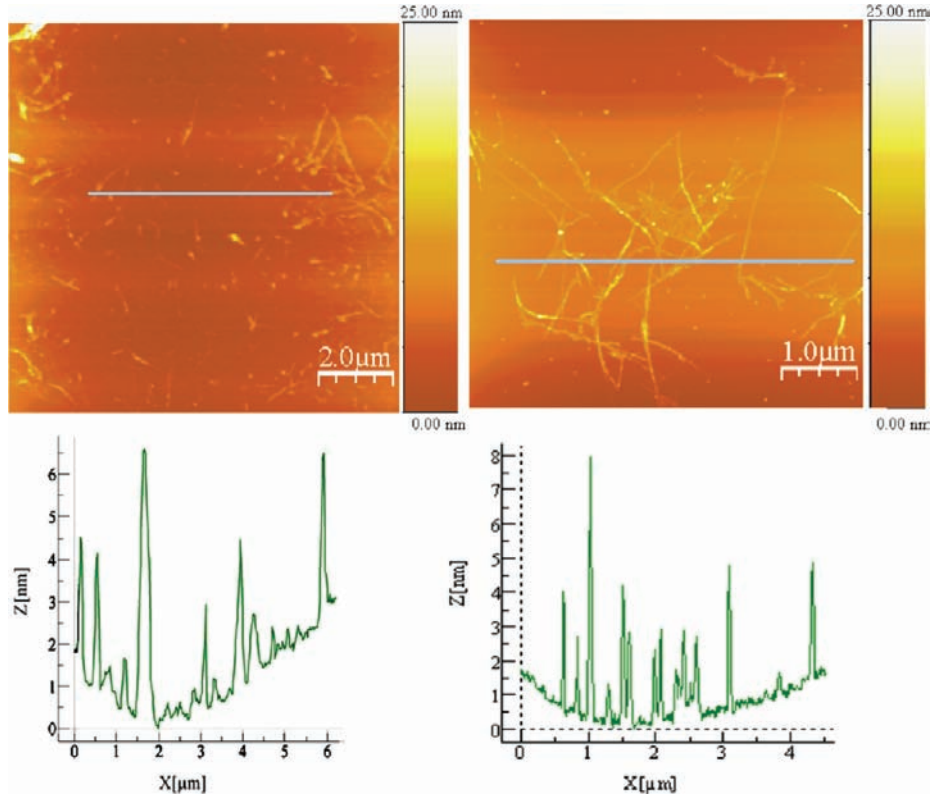

Figure 7. Tapping-mode AFM images (topography) of **ox-SWNT-Phe-O-*t*Bu** (left, 100 μm^2) and **ox-SWNT-TEG-NH-Boc** (right, 25 μm^2) dispersed in d_6-DMSO-saturated solutions and deposited on mica surfaces.

between linked and free HCl·H-Phe-O-*t*Bu. Therefore, in the diffusion time between the two gradient pulses, the signals arising from the fast-diffusing HCl·H-Phe-O-*t*Bu become strongly attenuated and disappear under the noise level. To verify that the signals observed in the ^{1}H and 1D DOSY NMR spectra of the derivatives arise from the solubilized ox-SWNT derivatives, we deposited the d_6-DMSO solutions of the conjugates onto copper grids for TEM inspection. Using this technique, it was possible to collect several images, such as those reported in Figure 6.

In these images, it is possible to detect many bundled ox-SWNTs, with lengths of approximately 1 μm, and some isolated ox-SWNT derivatives with lengths of a few hundred nanometers. The same d_6-DMSO solutions were then deposited onto clean mica surfaces to perform tapping-mode AFM characterization. The spin-coating (3000 rpm for 3 min) of one drop ($\sim$50 μL) of those saturated solutions easily allowed the identification of objects on the mica surfaces, without need to increase the deposition amount or dilute the solution before spin-coating. Figure 7 shows two images of a portion of the mica surface

spin-coated with **ox-SWNTs-Phe-*t*Bu** and **ox-SWNT-TEG-NH-Boc**, with their related cross section analysis (for additional images collected at different areas, see Figure S4 in the Supporting Information).

The cross section analysis of the AFM images indicates that some of the observed objects show less than 2 nm of height. Taking into account the deconvolution of the tip and that ox-SWNTs are enriched in semiconducting (characterized by larger diameters) nanotubes, these values are consistent with the presence of isolated, relatively short SWNTs. Nevertheless, the majority of the objects covering mica surfaces shows cross sections between 2 and 10 nm, which suggests the presence of bundles composed by few (2−8) nanotubes (Figure S3 in the Supporting Information).

Conclusions

We report for the first time the application of a diffusion-based NMR experiment (1D DOSY) for the characterization of covalently modified CNT derivatives. The DOSY results taken together with the Kaiser test support the formation of covalent derivatives of ox-SWNT, with ^{1}H NMR signals characteristic of the functional groups used in the derivatization but with a diffusion behavior typical of a macromolecular system. Despite the low number of functionalities attached to the CNTs, attenuation of interfering signals by the DOSY sequence allows the detection of ^{1}H NMR signals of the groups used for derivatization and thus to obtain structural information regarding the conjugates in a fast and reliable way. TEM and AFM characterizations demonstrate that the NMR observations are related to solubilized short SWNTs, indicating that this analytical approach can in principle be extended to other CNT derivatives, including functionalized multiwalled CNTs or non-oxidized SWNTs. The only limitation consists in the generally low dispersibility of CNT samples, which, even when functionalized, still exhibit a low solubility. In addition, the amount of organic moieties able to generate adequately intense ^{1}H NMR signals is low in relation to the overall molecular weight. However, this technique can become a very useful way for determining the molecular structure and the covalent attachment in functionalized CNTs.

Experimental Section

SWNTs produced by HiPco technique were purchased from Carbon Nanotechnologies, Inc. (lot no. R0510c) and oxidized by a two-step oxidative treatment as previously reported.[33]

General Procedure for the Activation of ox-SWNT. ox-SWNTs (50.0 mg, 170 μmol of COOH) were sonicated in a water bath for 20 min in DMF (15 mL) to give a black homogeneous suspension. Then DMAP (21.0 mg, 173.3 μmol) was added, and sonication continued for 10 min. NHS (61.2 mg, 521.1 μmol) was then added to ox-SWNTs dispersion, and sonication continued for 10 min. An additional solution of EDC·HCl (83.7 mg, 425.0 μmol) and DMAP (51.5 mg, 425.0 μmol) in DMF (5 mL) was slowly added to the ox-SWNTs dispersion. The reaction mixture was sonicated for 1 h and then stirred for 2 h and used without further purification in the subsequent steps.

General Procedure for the Preparation of ox-SWNT Derivatives. A 5-mL solution of HCl·H-Phe-O-*t*Bu or Boc-NH-TEG-NH_2 (425 μmol) and DMAP (425 μmol) in DMF was slowly added, under sonication (15 min), to the activated ox-SWNT-OSu. The resulting black suspension was stirred at room temperature for 36 h at room temperature to give **ox-SWNT-Phe-O-*t*Bu** and **ox-SWNT-TEG-NH-Boc** reaction mixtures. These suspensions were then precipitated with Et_2O (100 mL) and filtered under vacuum through 0.2-μm Fluoropore filters. The black precipitates were washed with Et_2O (100 mL) and dried under vacuum. The isolated products were then dispersed in DMF (10 mL) under sonication (10 min) and precipitated with Milli-Q H_2O (100 mL). Filtration through Isopore 0.2-μm filter yielded the derivatives as black powders that were washed with 0.1 M HCl solution (200 mL) and deionized H_2O (200 mL) to ensure complete removal of unreacted amines. The compact black precipitates were dried with MeOH under vacuum. Yields: **ox-SWNTs-Phe-*t*Bu** = 45.8 mg (91.6% w/w, 35% mol/mol, from TGA) and **ox-SWNT-TEG-NH-Boc** = 42.2 mg (84.4% w/w, 32% mol/mol, from TGA).

Preparation of the Mixture between ox-SWNTs and HCl·H-Phe-O-*t*Bu. ox-SWNTs (10.0 mg) and HCl·H-Phe-O-*t*Bu (2.75 mg) were sonicated in d_6-DMSO (10 mL) for 40 min. One milliliter of the supernatant was taken into a 3-mm NMR tube and subjected to ^{1}H NMR and 1D DOSY analysis.

Acknowledgment. This work was financially supported by the University of Trieste, INSTM, MIUR (PRIN 2006, prot. 200634372 and Firb, prot. RBNE033KMA1), the CNRS, the "Agence National de la Recherche" (ANR-05-JCJC-0031-01). We thank Mr. Claudio Gamboz for TEM assistance.

Supporting Information Available: Experimental procedures, detailing full characterization of the new compounds. This material is available free of charge via the Internet at http://pubs.acs.org.

JA902728W